Comparison of computational and experimental results for a transonic variable-speed power-turbine blade operating with low inlet turbulence levels

David Booth[1] and Ashlie Flegel[2]

[1]U.S. Army Research Laboratory – Vehicle Technology Directorate

[2]NASA Glenn Research Center

AIAA 51st Joint Propulsion Conference, Orlando, FL, July, 2015

Contents

- Motivation
- Experimental Description
  - Test Blade
  - Measurement Description
- Computational Approach
- Results and Discussion
  - Turbulence and Transition Model Comparisons.
  - Grid Sensitivity Study
  - Cruise Angle
  - Take-off Angle
- Summary and Conclusions

Motivation

- Develop modeling and simulation capabilities of variable speed power turbine (VSPT) blade aerodynamics.

- The VSPT is a potential enabling technology for high speed tilt rotorcraft, where the power turbine speed is slowed down by as much as 51% during cruise flight compared to take-off (hover) flight.

- Significant design challenges exist for the VSPT blades due to this speed change, such as high work factors, transitional flow, and low aft stage Reynolds numbers at 28 kft cruise, and large incidence angle variations (40° to 60°).

- The predictive capability of the CFD++ code was assessed in terms of blade loading, loss, and turning through comparison with experimental results obtained by Flegel-McVetta *et al*., 2013, NASA TM-2013-218069, at the NASA Glenn Research Center Transonic Turbine Blade Cascade Facility.

Experimental Description

Data were obtained in NASA-GRC's Transonic Turbine Blade Cascade CW-22.

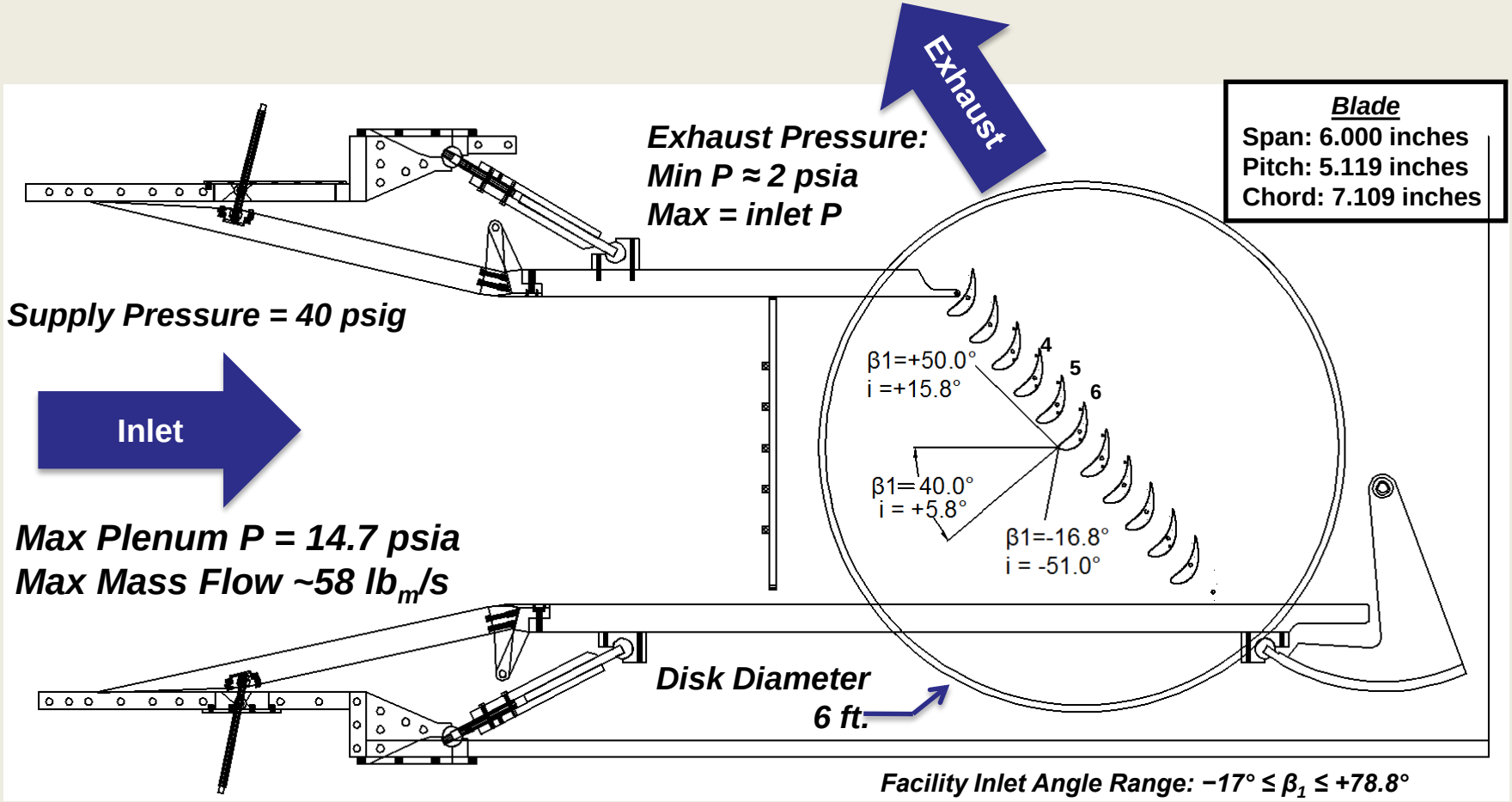

Test Blade

- VSPT midspan section blade, $\beta_{1,des}$= 34.2°
- Ten incidence angles tested: +15.8° to −51.0°
- 5 flow conditions each
- Inlet boundary layer range: 1.16 -1.69 inches (39% - 56% of half-span)
- No turbulence grid installed: (*Tu* = 0.24% - 0.40%, Λ = 1.0 – 1.5 inches)

Geometry	Value
Axial Chord, C_x	180.57 mm (7.109 inches)
True Chord	194.44 mm (7.655 inches)
Pitch, S	130.00 mm (5.119 inches)
Span, H	152.40 mm (6.000 inches)
Throat Diameter	72.85 mm (2.868 inches)
Leading Edge Diameter	15.16 mm (0.597 inches)
Trailing Edge Diameter	3.30 mm (0.130 inches)
Stagger Angle	20.35°
Inlet Metal Angle	34.2°
Uncovered Turning	19.47°
Exit Metal Angle	−55.54°

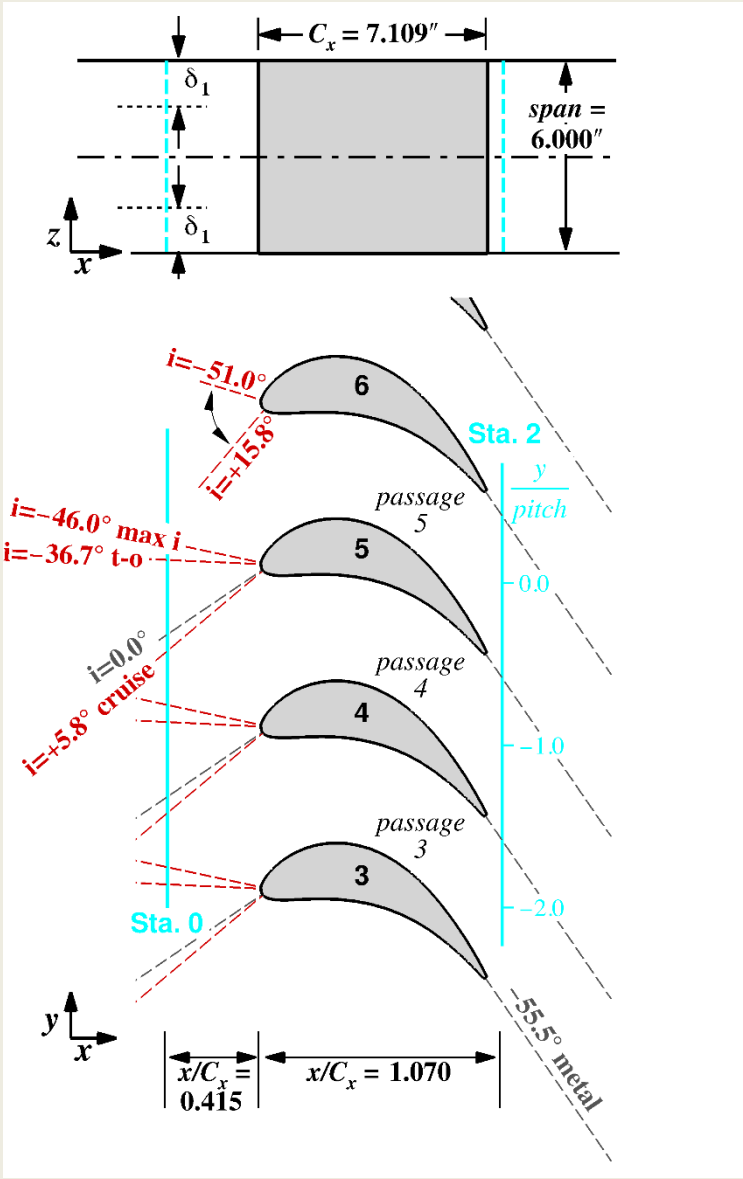

The Nation's Premier Laboratory for Land Forces

Measurement Description

- Total pressure and exit flow angles measured 7% C_x downstream of trailing edge. Detailed flowfield surveys were obtained at 26 spanwise locations.
- Blade and endwall static pressure measurements
- Two cases representing cruise and take off were documented in detail and are used for this assessment.

Angle and Flow Conditions Used in Simulations.

Incidence Angle, i	Inlet Angle, β_1	Inlet Re_{Cx}	Exit Re_{Cx}	Pressure Ratio	Exit M_{is}	δ_{inlet} in.
−36.7° (Takeoff)	−2.5°	294,700	527,400	1.35	0.67	1.50
+5.8° (Cruise)	+40.0°	389,100	531,000	1.41	0.72	1.44

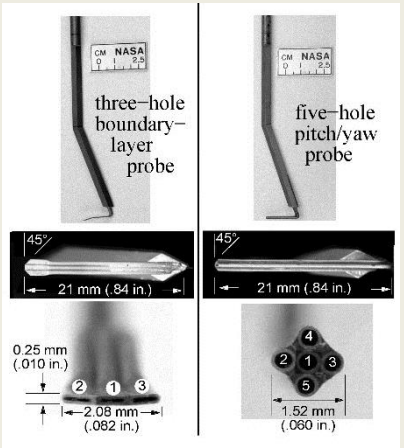

3-hole and 5-hole Probe Description

Computational Approach

- Flow Solver
  - 3-D steady-state (RANS) and time-resolved (URANS) computations were conducted using CFD++ version 14.1, which offers flexibility in terms of turbulence and transition modeling options.
  - The selected equation set was a pressure-based compressible perfect gas Navier-Stokes solver.
  - The spatial discretization used by the code is a multi-dimensional Total Variation Diminishing (TVD) polynomial interpolation determined through limited reconstructions over cells and/or nodes. Spatial discretization is second order with node based polynomials.
  - The local Courant number is used to accelerate convergence and second order dual time stepping technique is selected for time accurate computations.

- Computations were run in parallel on a Department of Defense Supercomputing Resource Center (DRCE) supercomputer.

Computational Approach

- CFD Mesh
  - A 3-D multi-block structured mesh generated from the experimental blade coordinate data.
  - One half of the blade span was modeled.
  - Periodic boundary conditions were used for the upper and lower boundaries of the grid.
  - Grid was rotated about the center of the blade in the z-direction in order to change the incidence of the blade with respect to the incoming flow.
  - A Musker inlet velocity profile boundary condition was used to correctly specify the spatial variation in both turbulence energy and length scale and match the experimental inlet conditions.

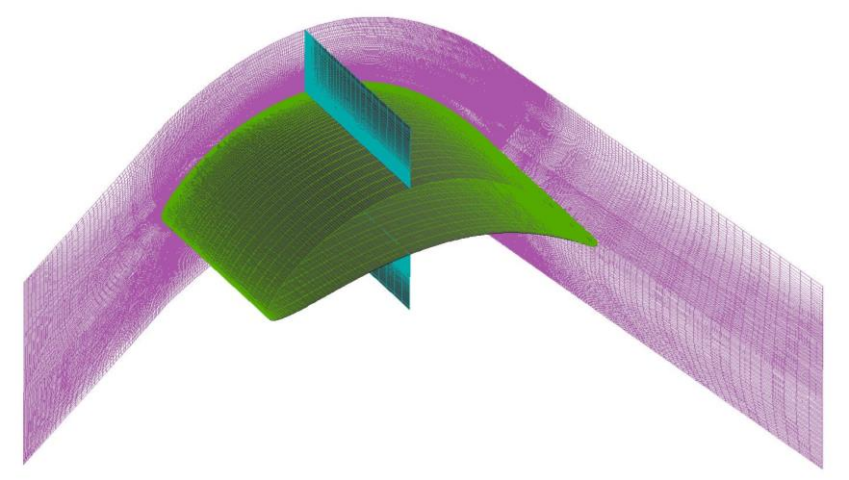

Computational Approach

- To accurately resolve the viscous boundary layer of the end wall, a boundary layer grid was created with a maximum thickness at the exit boundary plane of the grid that was estimated using a one-seventh power law equation for turbulent flow on a flat plate and the experimental boundary layer estimate, which was measured close to the inlet plane of the grid.

- An initial distance from the wall to the first wall-adjacent centroid of 3.0×10^{-5} inches was chosen to obtain a y + on the order of 1 at the boundary layer edge

- A tanh boundary layer spacing was used with a 1.1 expansion factor. The cell height outside the boundary layers was also gradually increased using a tanh function.

- A low turbulence intensity level of 0.325% was used to match experimental estimations.

- A turbulence length scale of 0.3% of the span was used as calculated by Ameri et al., NASA/TM—2013-217860.

Turbulence and Transition Model Comparisons

- RANS solutions were obtained using the two-equation realizable k-epsilon model, two-equation Shear Stress Transport (SST) model, and four-equation Langtry-Menter model.

- An algebraic transition prediction model, “Algebraic I”, was used in conjunction with the realizable k-epsilon turbulence model. A second algebraic transition model, “Algebraic II”, was used with the SST turbulence model. The Langtry-Menter model is a transition prediction model.

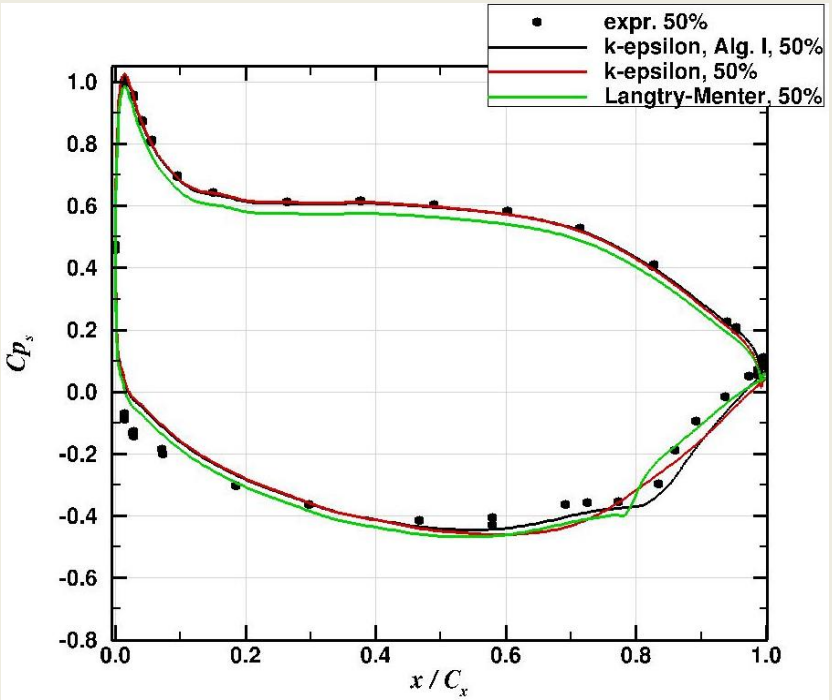

Turbulence and transition model comparison for cruise condition midspan pressure distributions.

- The k-epsilon and Algebraic I model and the Langtry-Menter model had the best agreement with the data for previous airfoil examples tested with the code.

- Overall, the k-epsilon turbulence model with the algebraic transition model I matched best to experiment for pressure distribution and was used for the remainder of this study.

Turbulence and Transition Model Comparisons

- A comparison of skin friction predictions on the suction surface at midspan for the cruise condition was made for all models.
- All three transition models appear to show separation occurring prior to the transition.
- Experimental data was not available to compare to the skin friction predictions.

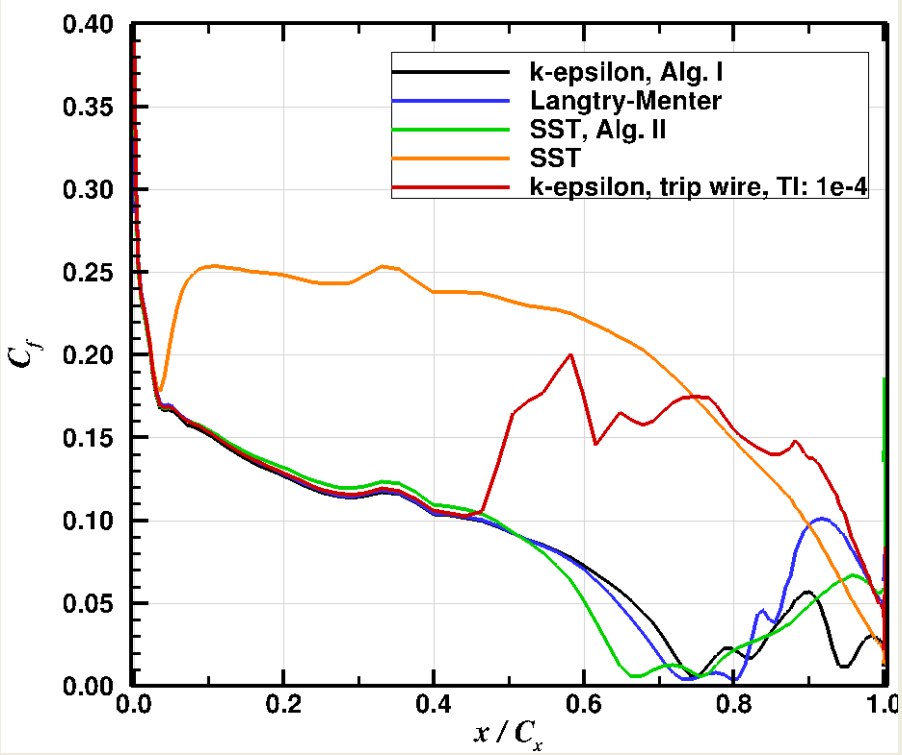

Comparison of skin friction predictions of several turbulence and transition models.

Grid Sensitivity Study

- Three grids were constructed starting with 8 million cells and progressively coarsening the grid to 4 and 2 million cells.
- Grid coarsening was uniform in all directions from one coarsening to the next.
- Mesh quality decreased, measured by increasing skewness and aspect ratio, as coarsening occurred.
- Observed sensitivity of accuracy of results to change from 8 million to 2 million grid points in the resolution of fluid flow scales in the chordwise, spanwise, and pitchwise directions.
- It was demonstrated that solution results were independent of grid refinement at 4 million points, with the 4 and 8 million point grids producing similar results.

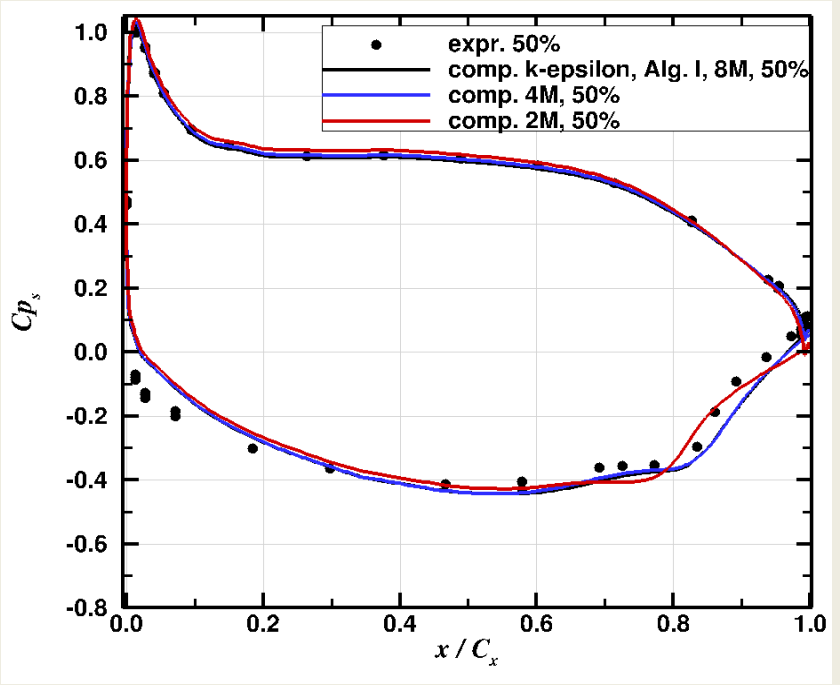

Comparison of grid resolution for cruise condition midspan pressure distribution predictions.

Cruise Angle Data

(i = +5.8°)

Blade Loading Comparisons

Blade Pressure Distributions

- Comparisons were made of RANS computations to experiment for cruise condition pressure distributions at four spanwise locations.
- Overall good agreement is observed between the computations and experimental data.
- At x/C_x = 0.7 - 0.9 the computations predict the suction side separation/reattachment at midspan suggested by the experimental data (black circles).

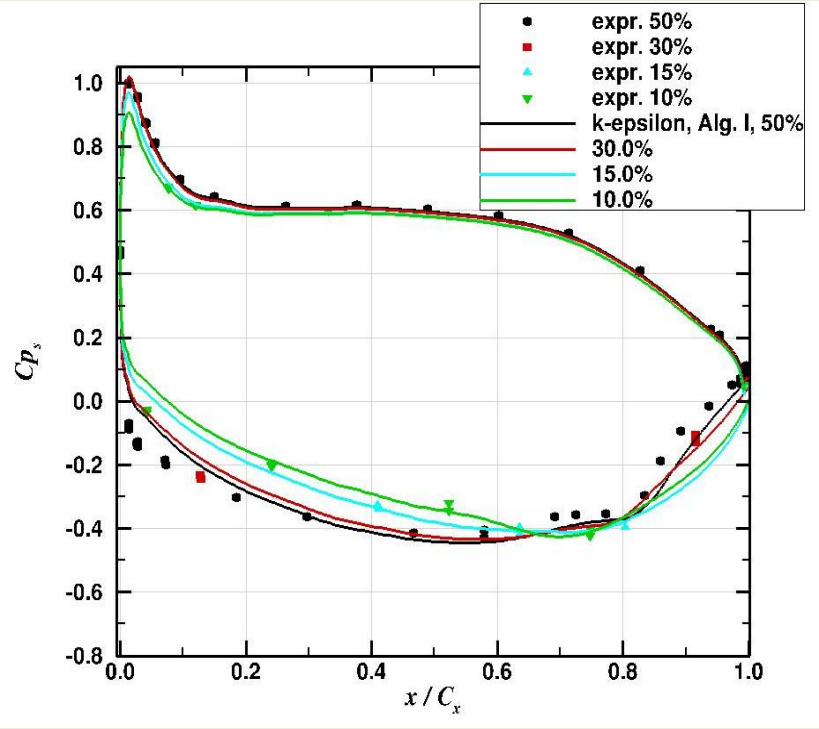

Skin Friction

Skin Friction Plots At Four Spanwise Locations

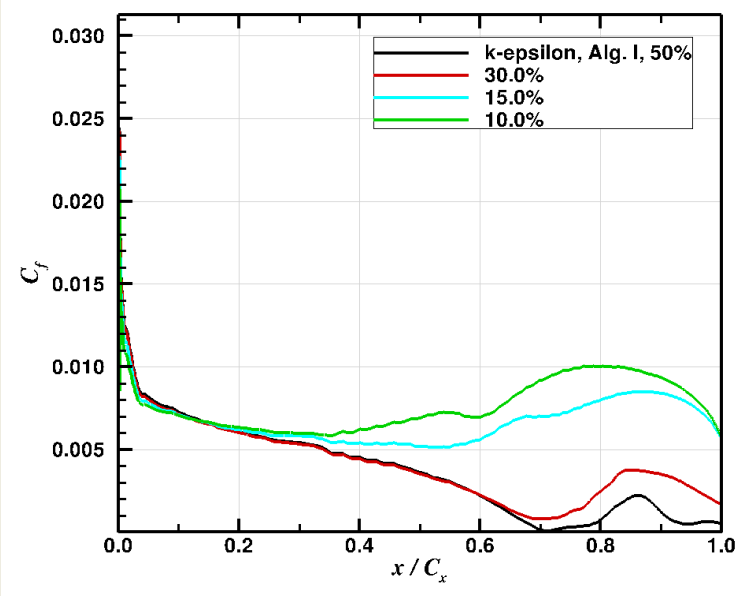

Suction side

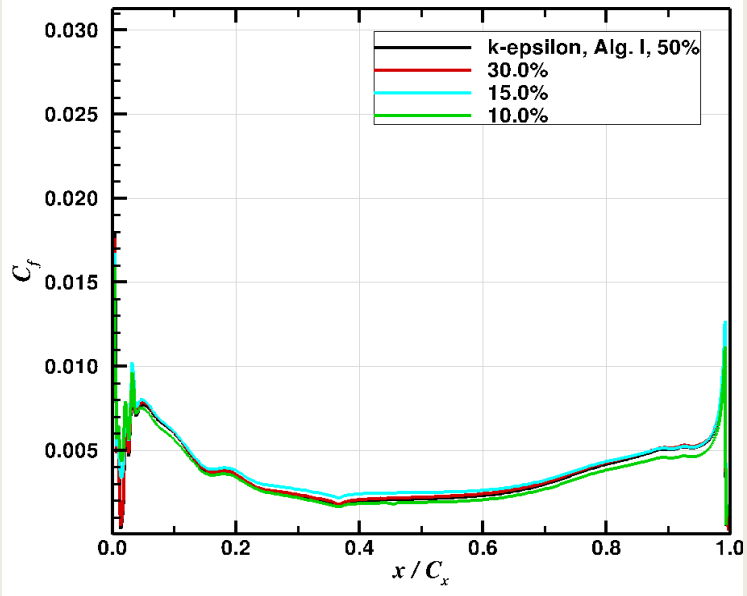

Pressure side

- Separation predicted on the suction side at midspan at an axial location of 70% with reattachment at around 80%. The area of separation predicted by the code matches the inflection in the experimental pressure distribution.
- Transition on the suction side is very three dimensional in the spanwise direction.
- The pressure side appears to predict a long transition before the flow becomes turbulent.

Cp_t contours

Exit Total Pressure

- Agreement is good for the loss core due to the pressure side leg of the horseshoe vortex, corresponding to the experimental data at (-0.55, 0.38).
- Results over predict the loss core in the region of the wake of the blade, corresponding to the region (-0.55, 0.5) due to the separated flow in the vicinity of midspan.
- Results under predict the third loss core close to the hub due to the wake and endwall boundary layer interaction, corresponding to the region near (-0.5, 0.02).

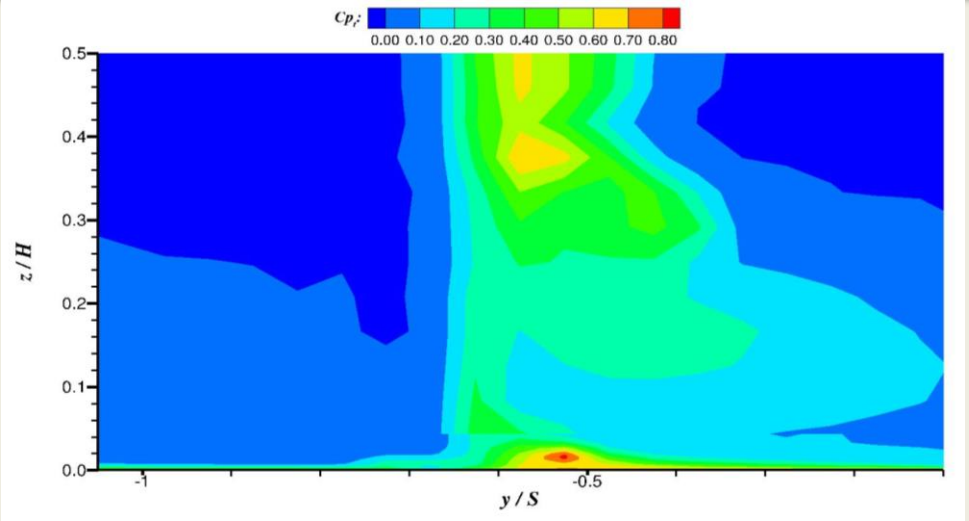

Experimental data

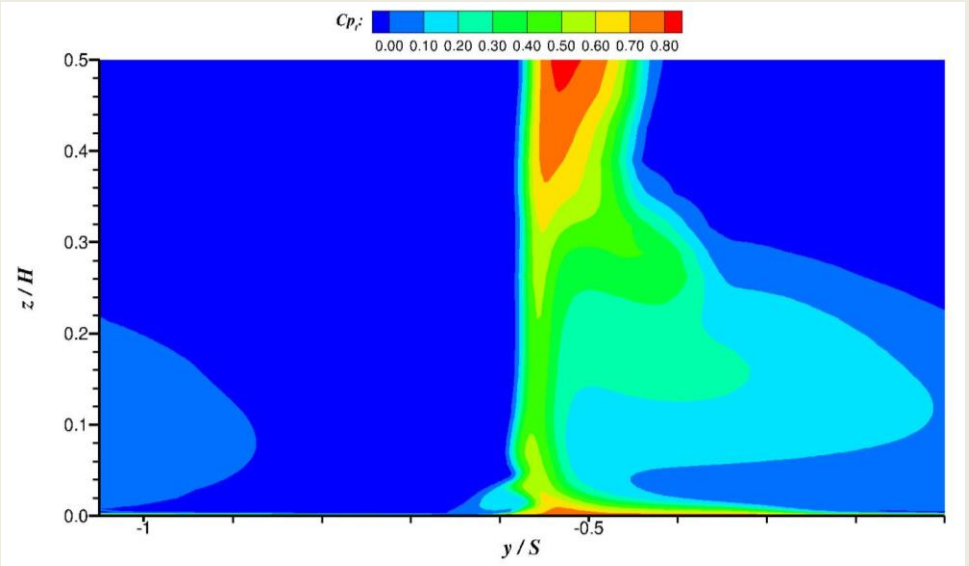

Computed

Midspan Total Pressures

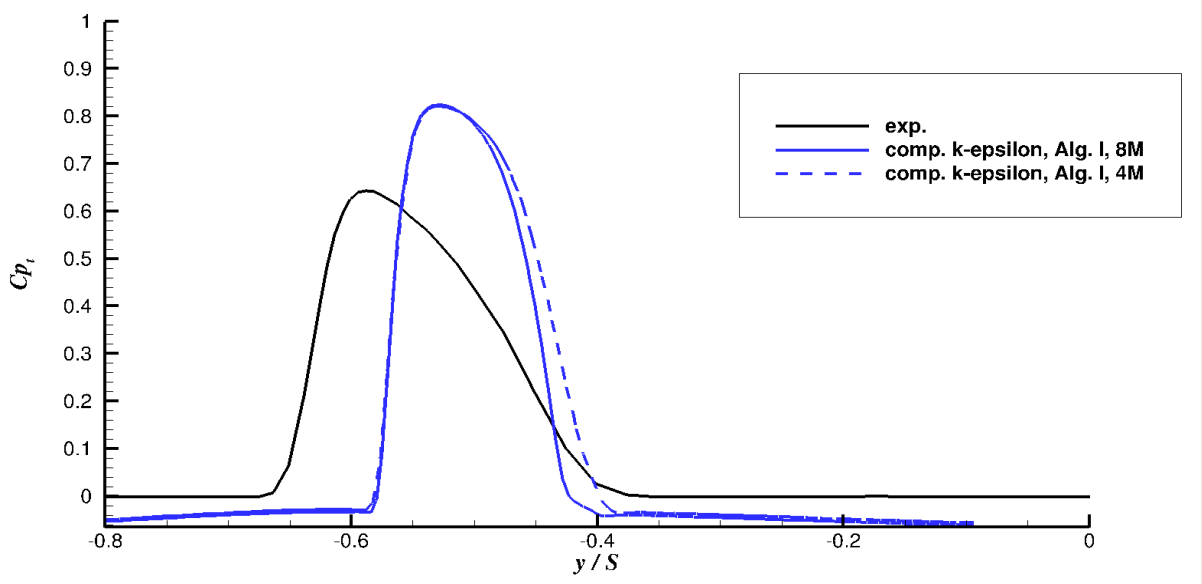

- The computations over predicted the maximum Cp_t value, and locate it slightly higher in pitchwise location.
- In addition computed values of Cp_t outside the wake are negative in value, which may be caused by numerical inaccuracy in the code.

Total Pressure Coefficient

Area-Averaged Total Pressure Coefficient Comparison

- Computational results mostly under predicted total pressure coefficient with agreement being very good up to *z/H* = 0.2 and the greatest difference occurring at approximately *z/H* = 0.38.

- This difference is likely due to the thinner wake predicted at that location for the loss core due to the pressure side leg of the horseshoe vortex.

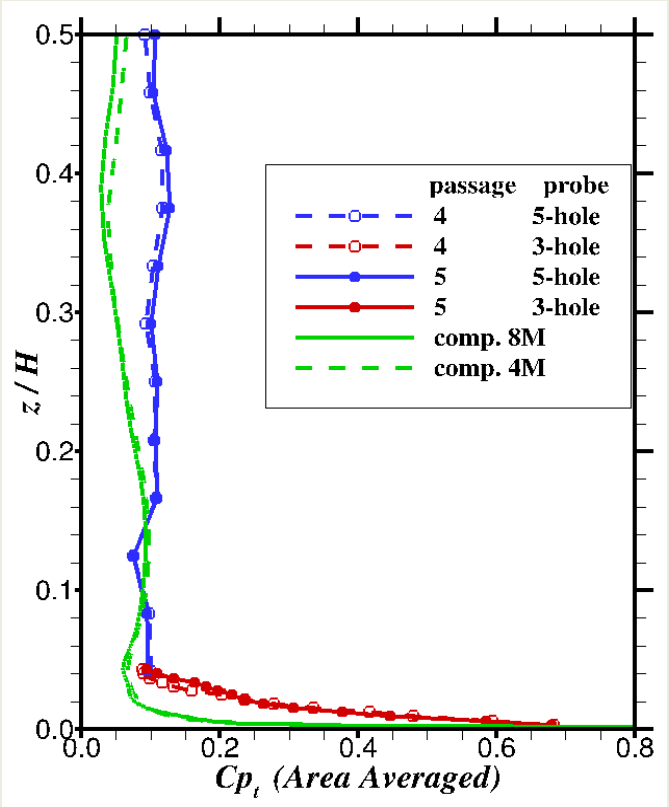

Pitchwise Exit Flow Angle

Exit Angle Comparison

- Agreement between experiments and computation is very good from *z/H* = 0.1 - 0.3 and then diminishes toward midspan.

- From *z/H* = 0.1 - 0.0, approaching the highly overturned region very near the endwall, agreement also diminishes.

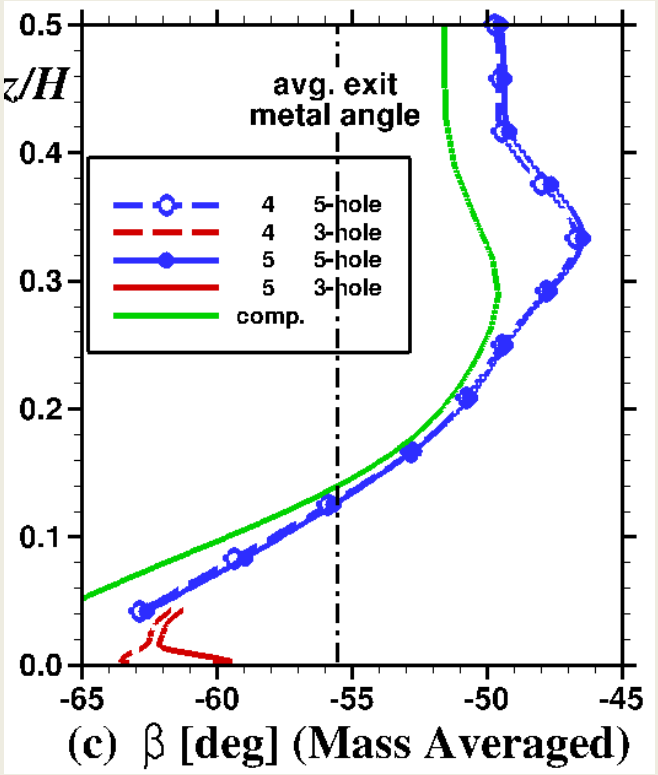

Takeoff Angle Data

(i = −36.7°)

Blade Loading Comparison

Blade Pressure Distributions

- Comparison of URANS computations to experiment for blade pressure distributions at four spanwise locations were made.
- The plots show good agreement between computations and experiment.
- On the pressure side computations reveal regions of separation across the span near the leading edge until x/C_x = 0.25 although there are not enough experimental data points to confirm if this is the case.

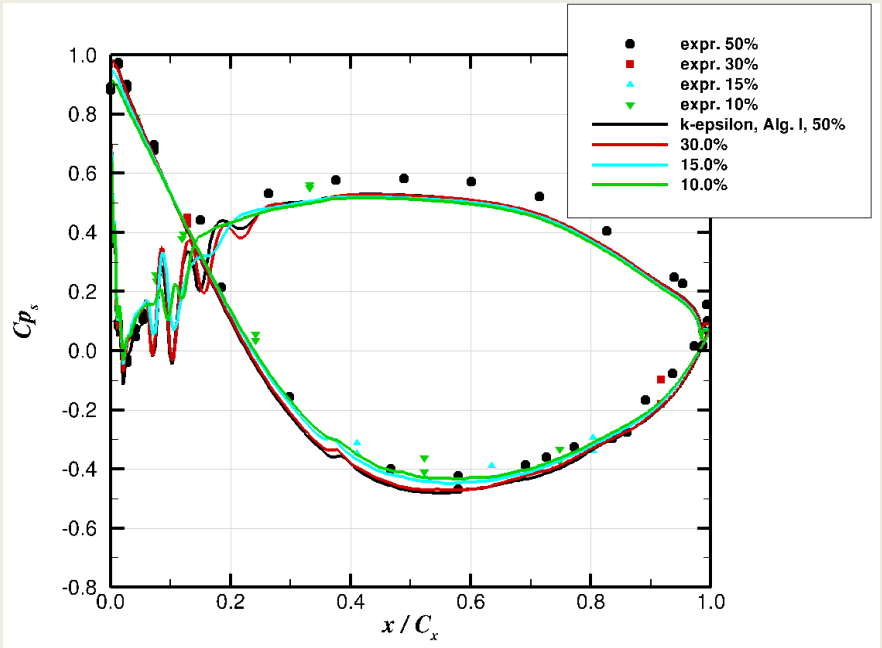

- On the suction side a slight plateau in the experimental data starting at x/C_x = 0.7, suggesting possible separation, is partially represented in the computational results.

Skin Friction

Skin Friction Plots At Four Spanwise Locations

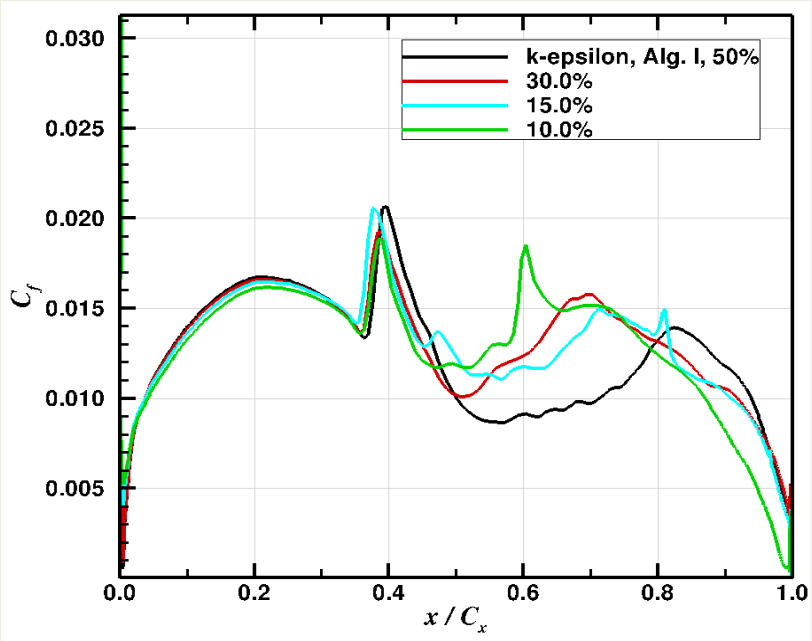

Suction side

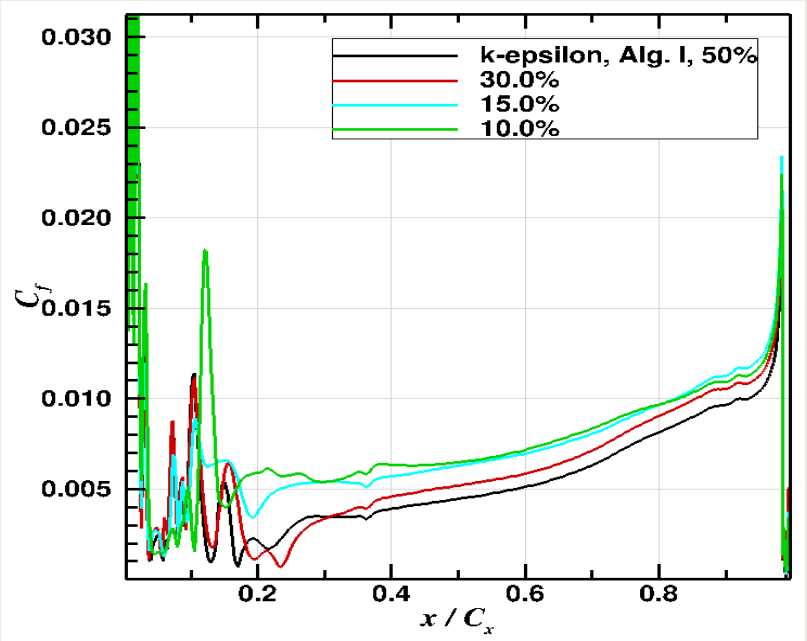

Pressure side

- For the suction side early transition is predicted at an axial location of 35%.
- There is reduced three dimensionality for transition location which is consistent with expectations as the blade is lightly loaded.
- For the pressure side several separation bubbles are suggested in the region close to the leading edge with transitioning to turbulent flow.

Cp_t contours

Exit Total Pressure

- Experimental data show the pressure side leg of the horseshoe vortex is present in the lower portion of the blade span at (-0.5, 0.14) due to the weakening of the passage vortex.
- The endwall wake interaction is still present in the same location as for the cruise condition (-0.5, 0.02).
- Computed results qualitatively match very closely with the measurements with these features located in the same regions.

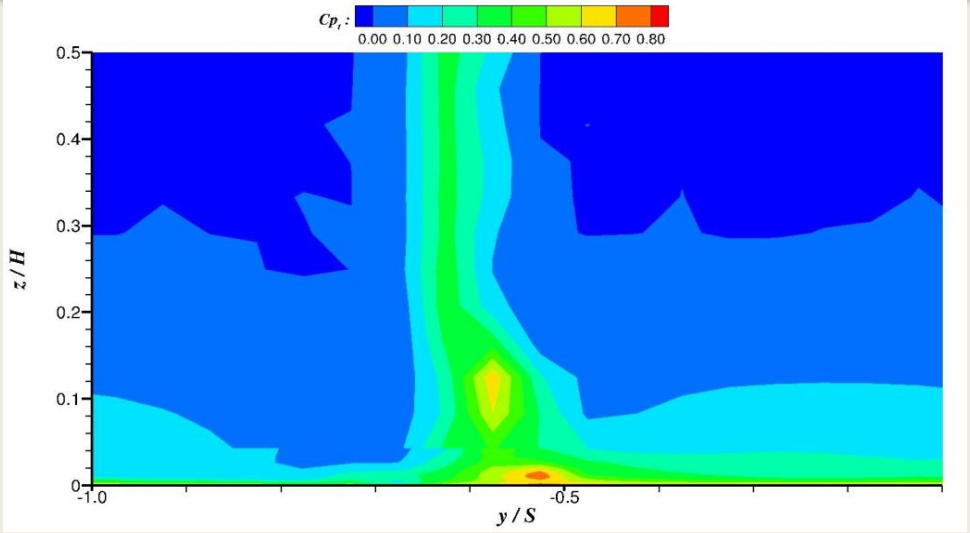

Experimental data

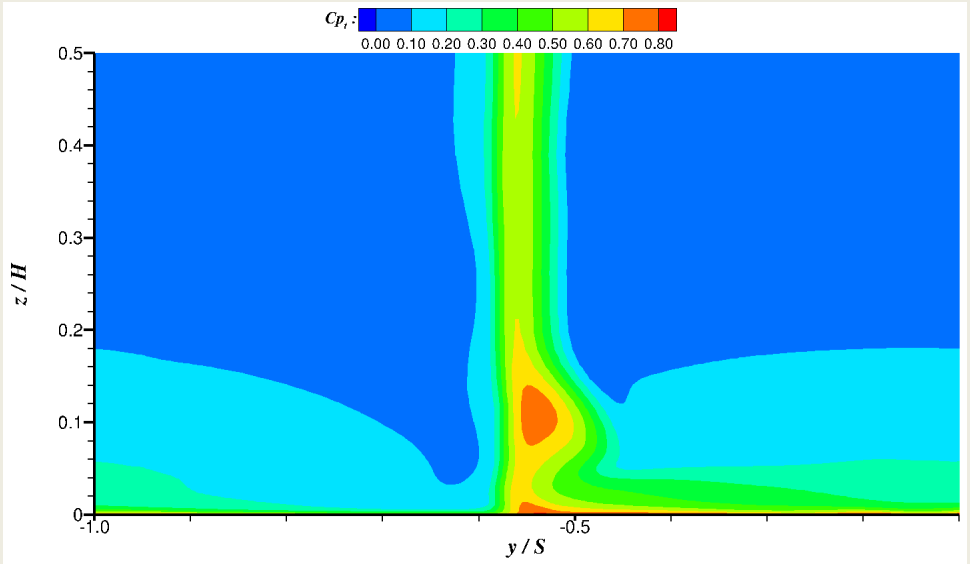

Computed

Midspan Total Pressures

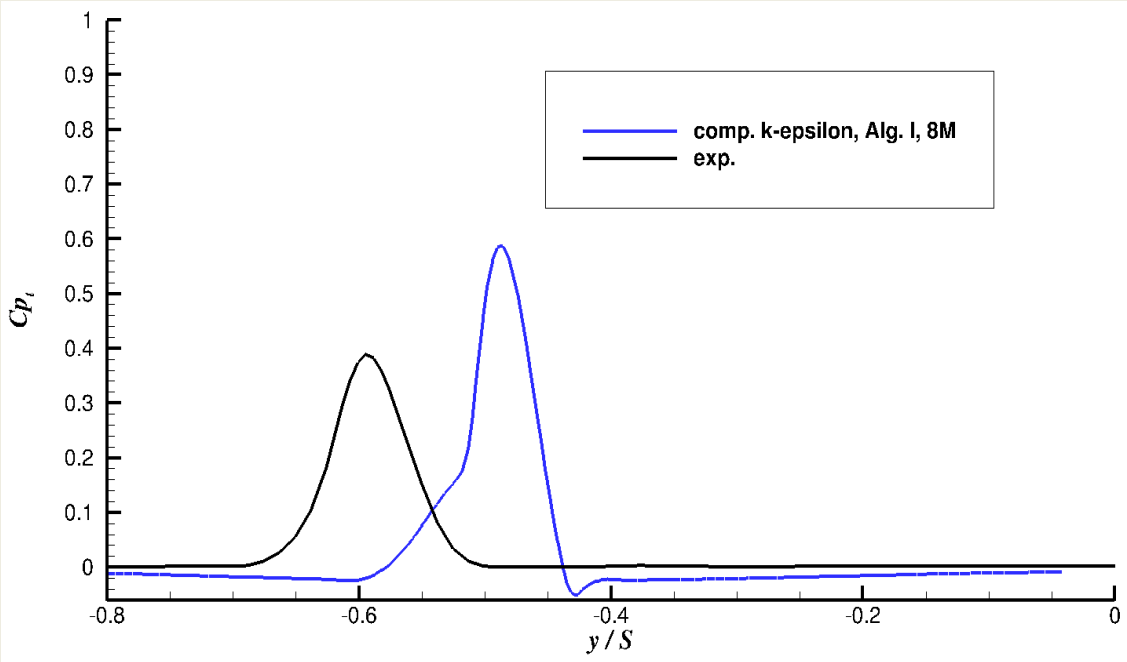

- The computations over predicted the maximum Cp_t value and there is some misalignment in the computed pitchwise location of the wake compared to measurements.

- These differences appear consistent with the differences in magnitude and location of the wake seen in the Cp_t contour plots at midspan.

Total Pressure Coefficient

Area-Averaged Total Pressure Coefficient Comparison

- Comparison of computational results to experiments is fair showing a qualitative similarity however the computational results consistently over predicted total pressure coefficient throughout the length of the plot away from the end wall region.

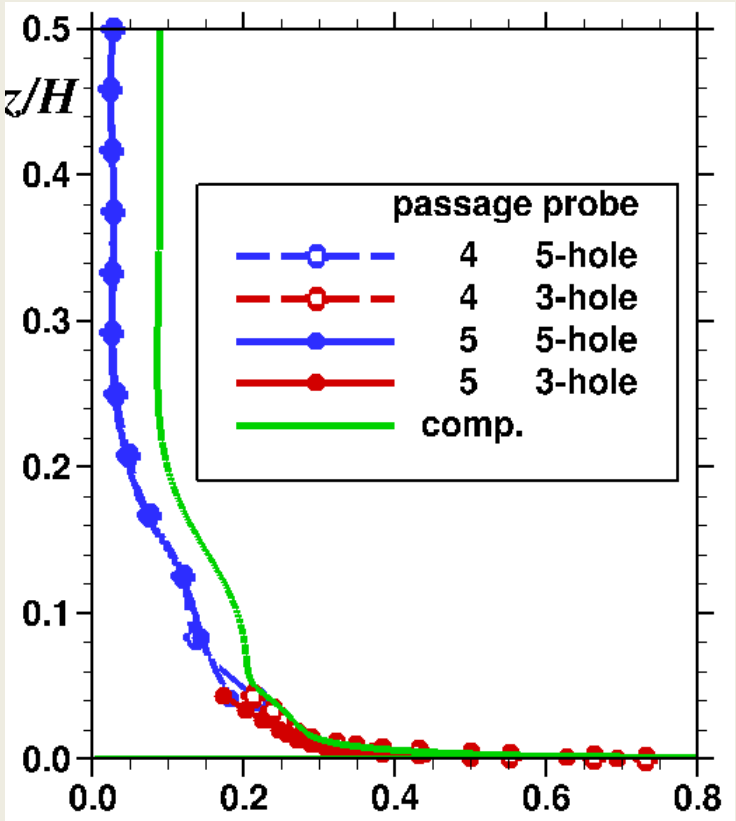

Pitchwise Exit Flow Angle

Exit Angle Comparison

- Agreement between experiments and computations is very good with differences being no more than 2^{o} except from z/H = 0.02 - 0.08 where differences are approximately 2.5^{o}, which is slightly outside the uncertainty range of the experiments.

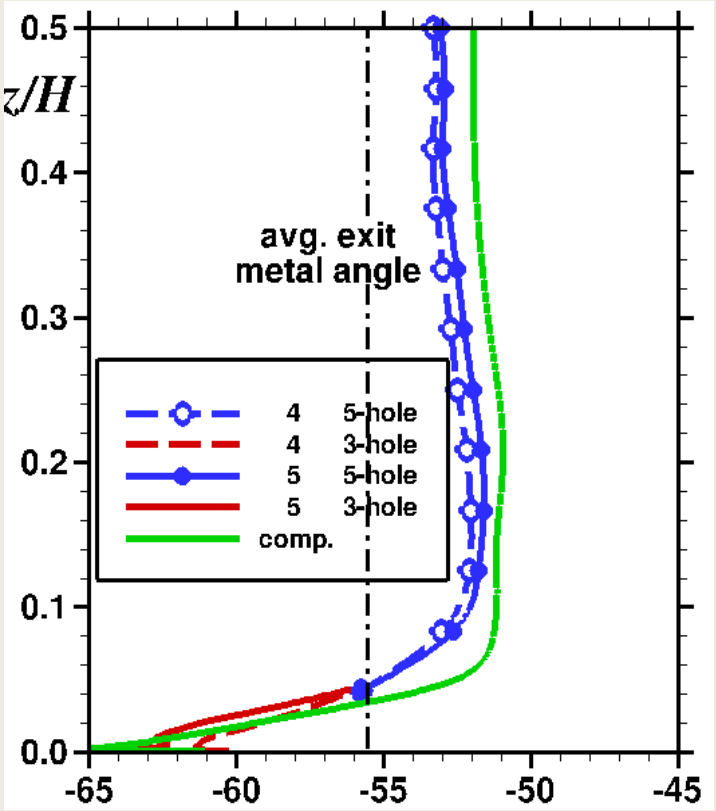

Summary and Conclusions

- Evaluation of the predictive performance of a COTS software code, CFD++, was performed using experimental data provided by Flegel-McVetta *et al*., 2013, NASA TM-2013-218069, of a VSPT blade midspan section tested in a transonic linear cascade.

- CFD computations were obtained at two blade incidence angle conditions corresponding to the turbine cruise design point condition and the take-off design point condition.

- The CFD code was assessed in terms of blade loading, loss, and turning against test data from the transonic tunnel.

- Computations of the three dimensional blade loadings agreed with the data for both conditions and were able to capture laminar separation on the aft 30% of the suction side for the cruise condition.

- For the total pressure survey downstream of the blade, agreement with the data was very good close to the end wall and diminished toward midspan.

Summary and Conclusions

- Agreement with the exit flow angle measurements was fair for the cruise angle and good for the take-off angle.
- Overall the CFD++ code and grid technique showed fair to good results compared to experiment for the VSPT blade.
- The combined k-epsilon turbulence model and algebraic transition model I produced the closest overall agreement with experiment, although further model comparisons should be made in the future as the code develops more capability.
- Further assessment should be done to improve the understanding of the capability of turbulence and transition codes and to improve predictions.
- In addition comparisons at other Reynolds numbers should be made to understand sensitivity of results to Reynolds number changes.

Motivation for VSPT Technology

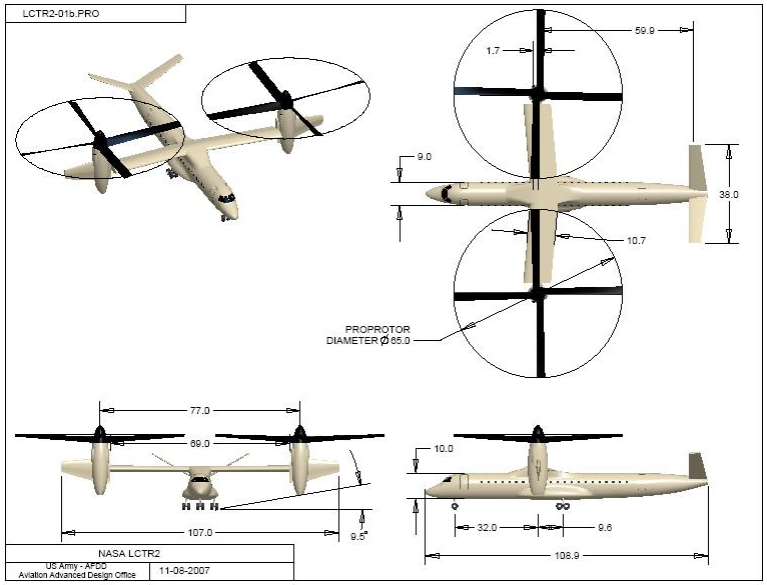

Acree, Hyeonsoo, and Sinsay, Int. Powered Lift Conf., 2008.

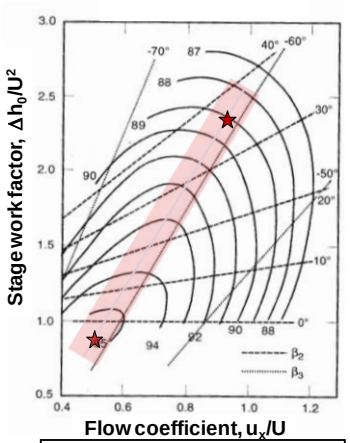

Smith chart

Large Civil Tilt-Rotor	
TOGW	108k lbm
Payload	90 PAX
Engines	4 x 7500 SHP
Range	> 1,000 nm
Cruise speed	> 300 kn
Cruise altitude	28 – 30 kft

Principal Challenge

Variability in main-rotor speed:
– 650 ft/s VTOL
– 350 ft/s at Mn 0.5 cruise

} ≈10 pts. in η_{prop}

Approaches

– Variable gear-ratio transmission
– Variable-speed power turbine **(VSPT)**
– or combination

VSPT Challenges

– Efficiency at high cruise work factor
  - $\Delta h_0 = D(u_q \cdot U) \approx$ const. at cruise and takeoff
  - $\Delta h_0/U^2$ cruise is 3.5 x takeoff

– 40^0 to 60^0 incidence angle variations in all blade row (and EGV) with 50% speed change

– Operation at low *Re* – transitional flow
  - 28 to 30 k-ft cruise leads to 60 k < $Re_{cx,2}$ < 100 k
  - Transitional flow